


## A NOVEL AND HIGH-THROUGHPUT APPROACH TO ASSESS PHOTOSYNTHETIC THERMAL TOLERANCE OF KELP USING CHLOROPHYLL $\alpha$ FLUOROMETRY<sup>1</sup>

Rosalie J. Harris ,<sup>2</sup> Callum Bryant 




Division of Ecology & Evolution, Research School of Biology, The Australian National University, Canberra, Australian Capital Territory, Australia

Melinda A. Coleman 

New South Wales Fisheries, National Marine Science Centre, 2 Bay Drive, Coffs Harbour, New South Wales 2450, Australia  
National Marine Science Centre, Southern Cross University, 2 Bay Drive, Coffs Harbour, New South Wales 2450, Australia  
Oceans Institute and School of Biological Sciences, University of Western Australia, 35 Stirling Highway, Crawley, Western Australia 6009, Australia

Andrea Leigh 

School of Life Sciences, University of Technology Sydney, PO Box 123, Broadway, New South Wales 2007, Australia

Verónica F. Briceño , Pieter A. Arnold , and Adrienne B. Nicotra 

Division of Ecology & Evolution, Research School of Biology, The Australian National University, Canberra, Australian Capital Territory, Australia

Foundation seaweed species are experiencing widespread declines and localized extinctions due to increased instability of sea surface temperature. Characterizing temperature thresholds are useful for predicting patterns of change and identifying species most vulnerable to extremes. Existing methods for characterizing seaweed thermal tolerance produce diverse metrics and are often time-consuming, making comparisons between species and techniques difficult, hindering insight into global patterns of change. Using three kelp species, we adapted a high-throughput method – previously used in terrestrial plant thermal biology – for use on kelps. This method employs temperature-dependent fluorescence ( $T-F_0$ ) curves under heating or cooling regimes to determine the critical temperature ( $T_{crit}$ ) of photosystem II (PSII), i.e., the breakpoint between slow and fast rise fluorescence response to changing temperature, enabling rapid assays of photosynthetic thermal tolerance using a standardized metric. This method enables characterization of  $T_{crit}$  for up to 48 samples per two-hour assay, demonstrating the capacity of  $T-F_0$  curves for high-throughput assays of thermal tolerance. Temperature-dependent fluorescence curves and their derived metric,  $T_{crit}$ , may offer a timely and powerful new method for the field of phycology, enabling characterization and comparison of photosynthetic thermal tolerance of

seaweeds across many populations, species, and biomes.

**Key index words:** chlorophyll fluorescence; macroalgae; photosystem II; temperature stress; thermal biology

**Abbreviations:**  $F_0$ , minimal fluorescence;  $F_v/F_m$ , maximum quantum yield of PSII;  $T_{crit}$ , critical temperature of PSII;  $T-F_0$ , temperature-dependent fluorescence

With rising sea surface temperatures, predicted at 1–3°C before 2100 (IPCC 2021) and an increase in the frequency and intensity of marine heatwaves (Oliver et al. 2018), understanding temperature thresholds of marine organisms is needed to identify vulnerability, predict patterns of ecological change and inform management and conservation strategies (Coleman and Wernberg 2020, Wood et al. 2021, Davis et al. 2022, Eger et al. 2022). As such, there is a need for fast, reliable, and high-throughput quantitative approaches to measure temperature tolerance in marine systems and to standardize measures over large spatial and temporal scales. This is particularly vital for foundation seaweeds that underpin vast ecological, economic, and cultural values in marine ecosystems (Eger et al. 2022), but for which empirical measures of temperature tolerance are often lacking.

Both warming and the frequency and intensity of extreme temperature events, such as marine

<sup>1</sup>Received 14 September 2022. Accepted 17 October 2022.

<sup>2</sup>Author for correspondence: e-mail rosalie.harris@anu.edu.au.  
Editorial Responsibility: M. Roleda (Associate Editor)

heatwaves (Holbrook et al. 2020) have, and will continue to have, major impacts on seaweeds (Harley et al. 2012, Sunny 2017), including local extinctions and declines (Vergés et al. 2016, Thomsen et al. 2019, Davis et al. 2022) and total reorganization of ecosystem structure (Vergés et al. 2014). For example, warming and heatwaves have caused local extinction of dominant kelps such as in *Durvillaea* spp. in New Zealand (Thomsen et al. 2019), *Ecklonia radiata* on the east and west coasts of Australia (Vergés et al. 2016, Wernberg et al. 2016), and range contraction of *Macrocystis pyrifera* forests in Baja California and Tasmania (Johnson et al. 2011, Cavanaugh et al. 2019). Similarly, cold snaps are also predicted to increase, and may have large impacts on intertidal species in polar and subpolar systems (Becker et al. 2009, Scrosati and Ellrich 2018). Cold snaps during the shoulder seasons when frosts and sea ice can occur earlier or later in the season can result in extracellular ice formation leading to cell death and inhibition to growth and development (Davison et al. 1989, Zhu et al. 2022). It is, therefore, necessary to investigate seaweed tolerance to both extreme heat and cold, to understand global patterns and drivers of seaweed losses and to be able to predict the future vulnerability of these important habitats.

Seaweed thermal tolerance has traditionally been measured using a wide variety of methods and many different response variables, making comparisons among different species, places and studies difficult. Techniques range from measuring gas exchange, biomass accumulation the use of chlorophyll fluorometry (Xiao et al. 2015, Sava et al. 2018) with response variables from oxygen concentration, relative growth rates and photosynthetic maximum quantum yield ( $F_V/F_M$ ). While different techniques are likely appropriate for specific studies, the wide variety of methodologies means there is currently no comparative, standardized metric or thermal threshold value that can be assessed across species, seasons, latitude, and other variables of interest. For seaweeds there is a lack of insight into global thermal physiological patterns as described for animals (Sunday et al. 2011) and more recently for land plants (Lancaster and Humphreys 2020). A streamlined, high-throughput approach to determine thermal thresholds would greatly enhance our ability to compare thermal thresholds and understand the relative vulnerability of seaweeds to temperature change.

Thermal tolerance in animals is often quantified by point of death or by changes in metabolic rate under a stress treatment, which are generally quite simple to detect (Roze et al. 2013, Caetano et al. 2020, Hall and Sun 2021). For photosynthetic organisms, the photosynthetic apparatus is an appropriate focus for thermal tolerance assays due to its sensitivity to temperature (Schreiber and

Berry 1977). However, in contrast to animals, it is difficult to determine either the point of death or the threshold for function of photosynthetic tissue through instantaneous visual detection. To tackle this issue, terrestrial plant ecologists and physiologists often use temperature-dependent chlorophyll fluorescence curves – generally defined as the rise in basal fluorescence,  $F_0$ , with an increase/decrease in temperature – to measure temperature sensitivity in plants within the photosynthetic apparatus (Schreiber and Berry 1977). Temperature stress results in the unfolding of photosystem II (PSII) protein complexes and the oxygen-evolving complex is denatured by the removal of manganese under adverse conditions (Enami et al. 1994). Temperature-dependent fluorescence ( $T-F_0$ ) curves provide a well-established way to measure heat or cold stress and thermostability of PSII (Ilík et al. 2003). This method has successfully been used to identify temperature thresholds of PSII and predict temperature sensitivity of species across varying latitudes, populations etc. Because it provides a mechanistic understanding of photosynthetic physiology in response to temperature, this method has enabled understanding of large-scale ecological patterns in land plants (Bilger et al. 1984, Knight and Ackerly 2002, O'Sullivan et al. 2017). For example, Knight and Ackerly (2002) compared congeneric species of desert versus coastal terrestrial plants between the field and glasshouse environments using metrics derived from temperature-dependent fluorescence ( $T-F_0$ ). They found no evidence to support that thermal tolerance of PSII was intrinsic across closely related genera from seed grown plants from desert and coastal environments, suggesting a high degree of plastic acclimation to the controlled environment they were grown in. As for the plants in the field, thermal tolerance varied more between species within a community than between congenics of desert and coastal genera suggesting that  $T-F_0$  parameters are more sensitive to the environment in which species occur than their phylogeny. Lastly, they found thermal tolerance of PSII was always lower in the glasshouse common environment (25°C day/15°C night) than in the field, indicating natural temperature fluctuations and extremes likely drive thermal tolerance higher to protect the plant.

Chlorophyll fluorometry has been applied to seaweeds broadly, with prior studies tending to focus on  $F_V/F_M$  (potential maximum quantum yield of PSII) as an instantaneous indicator of photosynthetic “health” or efficiency (Papageorgiou et al. 2007, Enríquez and Borowitzka 2010, Fernández et al. 2020). Although in some contexts  $F_V/F_M$  can be a useful indicator of various stressors, experiments using this metric tend to vary greatly in how long the photosynthetic tissue are exposed to set temperatures. There is also often variation in irradiance and how long a sample is given to acclimate or

recover, which make comparative measures across experiments difficult.  $F_V/F_M$  measurements are also time-consuming and often only capture a small subset of temperatures that individuals are exposed to, requiring interpolation, and thereby reducing precision. To date, assessment of  $T-F_0$  curves has not been attempted on seaweeds, but this approach holds great promise as a standardized and high-throughput metric for broad comparisons of thermal tolerance and thresholds. Because brown seaweeds and terrestrial plants have similarities in their light-harvesting pigment-protein complexes of PSII, with chlorophyll molecules phylogenetically related to each other (Caron et al. 2001), it is likely that this method can be used to assess the photosynthetic thermal tolerance of PSII of brown seaweeds. We expect that with examination into pigment compositions – note that red algae have the light-harvesting complexes outside of the photosynthetic membrane (Caron et al. 2001) – the method can likely be applied to many red and green algae species as well. Brown seaweeds are similar in their pigment to green plants in that they both share chlorophyll *a*, the pigment responsible for converting solar energy into metabolic energy and dissipating the excess of energy as fluorescence. Brown seaweeds do not have chlorophyll *b*, but have chlorophyll *c1* and *c2* (Etemadian 2017, Alam 2019) and have an increased antennae size in the light-harvesting complex adapted for low light conditions (Caron et al. 2001). Ultimately these pigments all function to deliver electrons to chlorophyll *a* reaction centers (Caron et al. 2001) and thus, measurements of PSII fluorescence in response to temperature should be applicable to seaweeds as they are to land plants.

When light energy is absorbed by a photosynthetic organism, it can be used for photosynthesis, it can be dissipated as heat, or it can be re-emitted as fluorescence (Maxwell and Johnson 2000). Each of these three fates is interlinked: a decrease in the efficiency of one will increase the yield of another. Chlorophyll *a* from PSII dominates chlorophyll fluorescence, especially minimal fluorescence ( $F_0$ ), which is the observable increase in fluorescence upon illumination, and thus, increases in fluorescence relate to the properties of PSII regarding energy conversion and excitation. Fluorescence yield can be used as an indicator of the efficiency of the photosynthetic apparatus as a whole (Schreiber and Bilger 1987). In temperature-dependent fluorescence curves, minimal fluorescence,  $F_0$ , is measured continuously under a weak measuring light while photosynthetic samples are being heated or cooled at a determined rate (Arnold et al. 2021). A steep fluorescence rise occurs when electron transport from the primary Quinone acceptor of PSII ( $Q_A$ ) to the secondary electron acceptor ( $Q_B$ ) is deactivated, indicating the onset of photosystem damage in response to temperature (Yamane

et al. 1997). This steep fluorescence rise can be calculated from the breakpoint between the slow and fast rise of  $F_0$ , which is referred to as the critical temperature ( $T_{crit}$ ) of PSII. Numerous studies use the term  $T_{crit}$ , thus to be clear, we are referring to the critical temperature,  $T_{crit}$ , as the onset of damage of PSII, which provides us with insight into the sensitivity of the thylakoid membrane to extreme temperatures (Bilger et al. 1984, Krause et al. 2010, Curtis et al. 2016, Zhu et al. 2018). Note that these rapid assays of  $T-F_0$  curves are indicators of temperature stress within the thylakoid membrane only during the heating/cooling treatment itself, and it cannot be assumed that irreparable damage has occurred (Bilger et al. 1984, Allakhverdiev et al. 2008). It is also important to note that the  $T_{crit}$  values derived from this method often exceed thermal tolerance limits cited in other work because the breakdown of PSII occurs after other physiological threshold processes have already begun. Further, the rate of change in temperature in the field can be as critical as its magnitude. Therefore, these are not “lethal limits” and should be viewed as relative values rather than absolute values, such that they provide a comparative metric of thermal tolerance useful for many macro-physiological and macro-ecological comparisons (Knight and Ackerly 2002, Curtis et al. 2016, O’Sullivan et al. 2017).

To accelerate research into the ecology and evolution of seaweed thermal tolerance, we developed an efficient, repeatable, and widely applicable thermal metric for seaweeds. Informed by terrestrial  $T-F_0$  methods, we applied a new method across multiple species of kelp and identify several important methodological considerations for application with species of differing thallus morphology or thickness. To optimize the use of  $T-F_0$  curves for the screening of thermal tolerance in seaweeds, we conducted several characterization experiments using three kelp species. These experiments aimed to characterize: (i) Decay of  $F_V/F_M$  of stored samples from time of collection, (ii) Optimal saturating pulse for use with kelps, (iii) Differences between  $F_V/F_M$  when measured using a Diving PAM and Maxi PAM (Maxi-Imaging-PAM (Pulse Amplitude Modulated); Heinz Walz GmbH, Effeltrich, Germany) and (iv) Effect of heating and cooling rate selection on kelp critical temperatures ( $T_{crit}$ ) of PSII. We reveal that this high throughput and efficient method could be widely adopted to support global research into the ecology and evolution of thermal tolerance in seaweeds and represents an important resource to predict the responses of seaweeds to changing temperatures.

## METHODS

*Species selection and sampling.* Three subtidal Phaeophyceae (brown seaweed) species were selected: *Phyllospora comosa*, *Ecklonia radiata* and a *Sargassum* sp., hereafter referred to as *Phyllospora*, *Ecklonia*, and *Sargassum*, respectively. These species are

the main habitat formers across south-eastern Australia (Coleman and Wernberg 2017, Wernberg et al. 2019) and differ in thallus shape, thickness, and size and thus represent a breadth of morphologies for optimizing this technique. Average thallus thickness was 0.89 mm, 0.64 mm, and 0.21 mm for *Phyllospora*, *Ecklonia* and *Sargassum*, respectively ( $n = 20$  per species). Species were collected on snorkel in approximately the middle of their latitudinal range, at Horseshoe Bay Beach, Bermagui, NSW, Australia (36°25'29.4" S, 150°04'46.3" E) in October 2021 for characterization experiments and to investigate the effect of heating/cooling rates on  $T_{crit}$ , and again in January 2022 to further test heating/cooling rates with changes in thermocouple placement. All samples were collected from ~2 m at low tide in the morning. The average water temperature was 16°C in October and 20°C in January. During collection, large sections from mid blades of healthy thallus were cut using secateurs and placed into moist cotton bags in a light-proof, black catch bag. On shore, samples were transferred to a cooler and transported to a laboratory within 10 min. On arrival to the laboratory, in a dimly lit room, eight thallus sections were cut into ~1 cm<sup>2</sup> sections per individual (same individual, different tissue used for multiple assays) and – to avoid tissue dehydration during the processing of other samples – placed into indexed pill boxes in the dark in the cooler. Preliminary assays showed that excised samples could be kept cut in these boxes under cool conditions for more than 12 h without a decline in  $F_V/F_M$ , a proxy assessing possible wounding effects (see Fig. S1 in the Supporting Information).

*Thermal tolerance measurements using temperature-dependent changes in chlorophyll fluorescence ( $T-F_0$ ) to obtain  $T_{crit}$  of PSII.* Following and adapting terrestrial plant methods from Arnold et al. (2021), thallus sections were placed onto a paper grid array of 30 cells, with a unique grid reference for each cell, before being covered with a sheet of plastic film wrap. Each sample was placed over a type-T thermocouple (Omega Engineering) to record temperature every 5 s using a dataTaker DT85 (Lontek, Glenbrook, New South Wales, Australia) with a layer of plastic film wrap between the thermocouple and the sample to avoid salt-corrosion of the thermocouple (Fig. 1). The array sat on top of a Peltier plate (CP-121HT; TE-Technology, Inc., Traverse City, Michigan, USA; 152 × 152 mm surface) that was controlled by a bipolar proportional-integral-derivative temperature controller (TC-36-25; TE-Technology, Inc.) and powered by a fixed-voltage power supply (PS-24-13; TE-Technology, Inc.). The plate was heated and cooled using four thermoelectric module points across the plate that can achieve a range from –20°C to 100°C if using a MP-3193 thermistor (TE-Technology, Inc.). Heating and cooling rates were controlled by an adapted version of LabVIEW software (National Instruments, Austin, TX, USA) using source code available from TE-Technology, Inc. based on the supplied user interface.

The samples were gently flattened against the plate and thermocouples with double-glazed glass to ensure good contact with thermocouples and to provide insulation to closely match the temperature of the Peltier plate and the samples (Fig. 1). Fluorescence parameters were measured using a Pulse Amplitude Modulated (PAM) chlorophyll fluorescence imaging system using the standard blue-diode (450 nm) light source (Maxi-Imaging-PAM; Heinz Walz GmbH). The fluorescence camera was mounted 185 mm above the Peltier plate to capture a total imaging area of 120 × 90 mm. Basal chlorophyll fluorescence ( $F_0$ ) was measured using a continuous weak blue pulse modulated measuring light (0.5 mmol photons · m<sup>-2</sup> · s<sup>-1</sup>) from the light-harvesting complex without driving photosynthesis in PSII (Schreiber and Berry 1977). Samples were dark-adapted for a minimum of 20 min to obtain minimal fluorescence ( $F_0$ ) and ensure that the

oxidized primary Quinone acceptor and non-photochemical quenching were inactive. Following dark adaptation, a saturating flash of 4000 μmol photons · m<sup>-2</sup> · s<sup>-1</sup> was applied to the samples to obtain maximal fluorescence ( $F_M$ ), variable fluorescence ( $F_V = F_M - F_0$ ) and their ratio ( $F_V/F_M$ ) as the potential maximum quantum yield of PSII (i.e., the quantum efficiency if all reactions centers were open; Maxwell and Johnson 2000).

After the saturating pulse, an image of the samples on the grid array could be viewed using the ImagingWin software (PC software ImagingWinGigE V2.56p), whereupon areas of interest were drawn over each sample to outline the largest region possible while avoiding the cut edges of the samples. To begin measurements, the modulated measuring light was turned on and the camera was set to record  $F_0$  every 20 s. Simultaneously, the Peltier heating/cooling program was set to the chosen heating/cooling rate and the dataTaker was turned on to record temperature every 5 s. The critical temperature ( $T_{crit}$ ) of PSII was derived from the breakpoint/inflexion point between the slow rise phase and the fast rise phase of  $F_0$  (Fig. 1c). These critical temperature values can be extrapolated as thresholds by which relative thermal tolerance can be compared across species, populations and seasons (Curtis et al. 2016, O'Sullivan et al. 2017, Zhu et al. 2018). Below, we detail several characterization experiments to adapt and optimize a  $T-F_0$  protocol used for terrestrial plants (Arnold et al. 2021) for use with kelps.

*Decay in  $F_V/F_M$  of stored samples from time of collection.* As our experiments required measuring  $T-F_0$  curves on multiple assays of samples, we first tested the most viable way to store the samples in the laboratory between assays. We tested the decay of the maximum quantum yield ( $F_V/F_M$ ) of samples stored in either seawater – that was changed every 24 h – or cotton bags wetted with seawater but not submerged, both stored in a dark cooler with a temperature of 16°C ± 1°C. Iterative  $F_V/F_M$  measures were taken from the intact thallus of five individuals per species held in each storage treatment for 100 h.  $F_V/F_M$  measurements were made using a Diving PAM (Heinz Walz, Effeltrich, Germany) using the ML-BURST mode.

*Saturating pulse optimization using the Maxi PAM.* A saturating pulse (intense flash of light) is applied to a dark-adapted sample to achieve  $F_M$  for calculating change in the ratio variable to maximum fluorescence (Maxwell and Johnson 2000). Studies vary widely in the intensity of the saturating flash that a sample is given to obtain  $F_V/F_M$  (Cabello-Pasini et al. 2000, Hüve et al. 2006, Arnold et al. 2021). The MAXI Version Imaging PAM M-SERIES (Heinz Walz GmbH) was designed for terrestrial plants that are adapted to high light environments relative to seaweeds. Hence, we optimized light settings to avoid photo inhibition of our samples while using a pulse strong enough capture maximal fluorescence. Samples from each of the three species were placed on the array under the PAM and exposed to one of a range of flash intensities (different array of samples per intensity setting). The units on the PAM are arbitrary and range from 1–10, Walz suggests setting 10 is 4000 μmol quanta · m<sup>-2</sup> · s<sup>-1</sup>. Regardless of unit, we sought to find the minimum saturating pulse that would give the highest  $F_V/F_M$  value with the least variation among samples and species. We tested five levels of intensity (Walz settings 2, 4, 6, 8 and 10) across three species with 10 replicates per species and, in our analysis, we used the middle setting (6) as the reference level for comparing  $F_V/F_M$  values.

*Comparison of diving PAM to Maxi PAM for measuring  $F_V/F_M$  of kelp.* Conventionally,  $F_V/F_M$  for seaweeds is obtained using a Diving PAM, but the Maxi PAM and Diving PAM are designed for different light spectrums and so the measurements are not directly comparable (from discussion with Walz

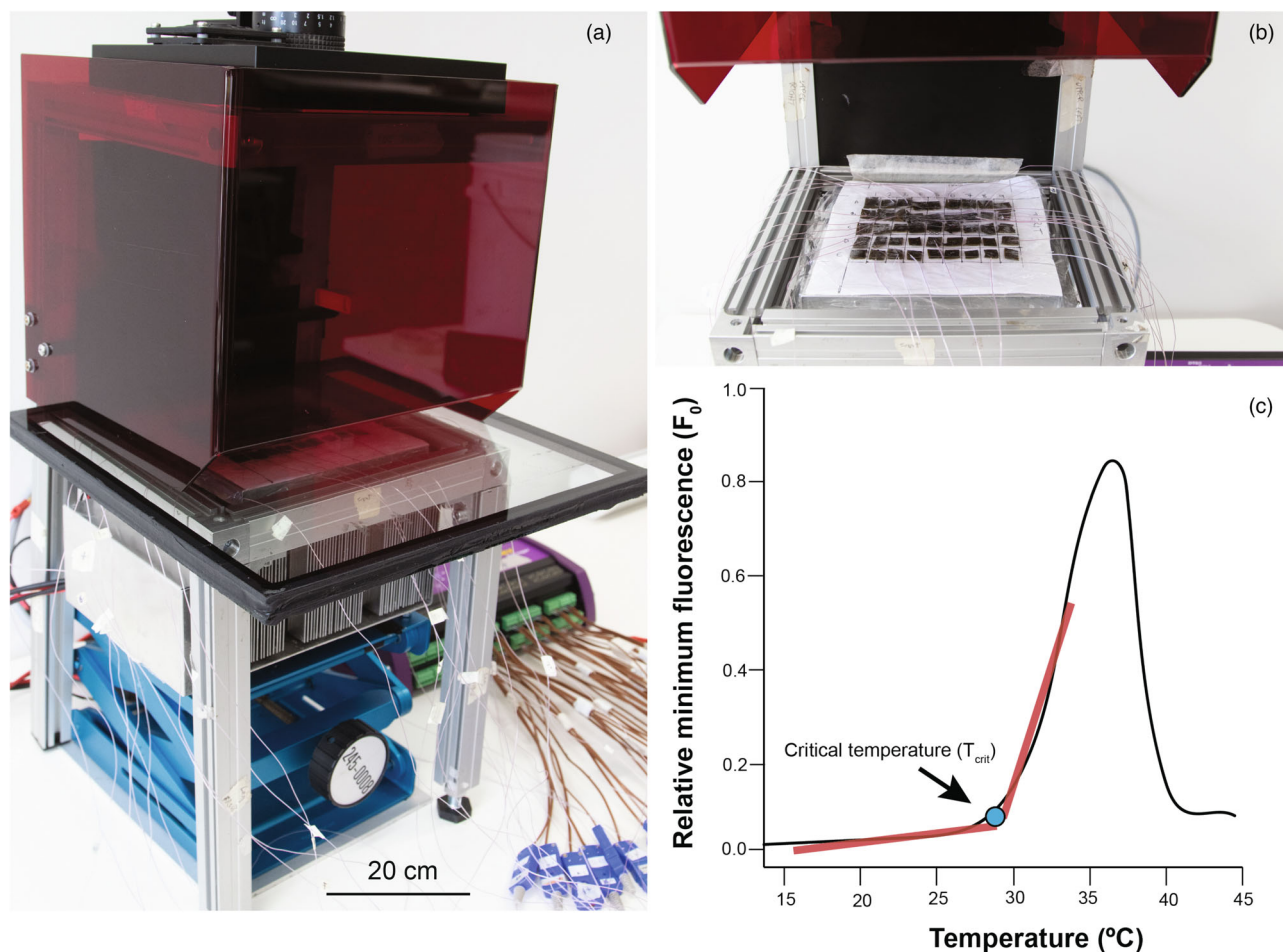


FIG. 1.  $T$ - $F_0$  setup and example fluorescence curve. (a) Imaging PAM (with red light shield) mounted with metal frame on top of the Peltier plate supported by a lab jack. Samples are compressed by double-glazed glass for contact with thermocouple and for temperature buffering. (b) Seaweed samples on array with grid references with a thin cover of plastic film with thermocouples attached to each sample. (c) Temperature-dependent fluorescence curve example showing the breakpoint/inflection between slow and fast rise fluorescence ( $T_{\text{crit}}$ ).

technical support). We tested the difference between the two types of PAMs using tissue cut from the same part of thallus and split in two, then plotted with a 1:1 regression to show the offset between the two types of PAMs.

*Effect of heating and cooling rates on  $T_{\text{crit}}$  of PSII of kelp species.* When measuring the  $T$ - $F_0$  curves, it is important to select heating or cooling rates that optimize the trade-off between high throughput and accuracy. The heating and cooling rates are also subject to different constraints both for the machinery and the tissue. Previous work on terrestrial plants suggests that the rate at which heating/cooling during the  $T$ - $F_0$  curve can significantly affect the measured  $T_{\text{crit}}$  of PSII value (Arnold et al. 2021). This is likely due to lag times in heating/cooling the leaf tissue too rapidly, inhibiting the time the leaf has to initiate protective mechanisms (Bilger et al. 1984, Frolec et al. 2008). Protocols for measuring heat tolerance tend to have a faster heating rate of around  $60^{\circ}\text{C} \cdot \text{h}^{-1}$  compared to cold tolerance studies, which often use much slower cooling rates (e.g.,  $5^{\circ}\text{C} \cdot \text{h}^{-1}$ ), though in many cases the choice of rate is arbitrary (Geange et al. 2021). We followed the same protocol as Arnold et al. (2021) to test the effects of different heating and cooling rates, where thermocouples were placed beneath the tissue samples and seven

rates (8, 15, 30, 45, 60, 120, and  $240^{\circ}\text{C} \cdot \text{h}^{-1}$ ) were compared for both heat and cold tolerance. We sought to identify the heating and cooling rates that generated consistent  $T$ - $F_0$  curves and  $T_{\text{crit}}$  values with minimal variation among species. Each heating/cooling rate began at the temperature from which the tissue had been collected (measured with HOBO Pendant Data Logger during collection,  $16^{\circ}\text{C}$  in October and  $20^{\circ}\text{C}$  in January). The heating/cooling rate assays were applied to the three species with 10 replicates per species and repeated three times over different times of day across multiple days for each rate. We analyzed the effect of heating and cooling rates on  $T_{\text{crit}}$  values across species, using  $60^{\circ}\text{C} \cdot \text{h}^{-1}$  and  $8^{\circ}\text{C} \cdot \text{h}^{-1}$  as respective reference levels against which the other rates were compared.

*Heating rate artifacts and modification of thermocouple placement for kelp species.* Analyses of the effects of heating and cooling rates from the above experiment revealed an increase in  $T_{\text{crit}}$  of PSII with rate (see Results). Large brown kelp thalli are thick and have high water content, and therefore, high thermal mass relative to most terrestrial leaves. We, therefore, posited that the placement of the thermocouple on the bottom of the sample may yield a discrepancy between measured temperature and the realized temperature at the thallus



surface, as it takes some time for the temperature of water-heavy tissue to reach equilibrium relative to the source temperature (Bell 1993, Djaeni and Sari 2015, López-Cristoffanini et al. 2015). The Maxi PAM measures fluorescence changes from the top of the sample and so it is likely overestimating  $T_{crit}$  of PSII if there is a lag time between when the bottom and top of the sample heat to a point of fast rise fluorescence. Therefore, to investigate this strong positive correlation of heating/cooling rate with  $T_{crit}$ , we repeated our previous experiment but added a thermocouple to both the top and bottom of the sample and calculated critical temperature for each side of the sample for heating rates only. In this repeated experiment, we included an additional heating rate of  $3^{\circ}\text{C} \cdot \text{h}^{-1}$  to ensure we captured a more complete range of rates.

*Testing the utility of  $T_{crit}$  as a comparative metric.* To briefly highlight the utility of  $T-F_0$  curves as a comparative and useful ecological metric, we compared a subset of the data from the previous experiment, collected in January 2022, to the initial data, collected in October 2021, for each of the three species at one heating rate of  $8^{\circ}\text{C} \cdot \text{h}^{-1}$ . At the time of collection these sites had sea surface temperatures of  $16^{\circ}\text{C}$  and  $20^{\circ}\text{C}$ , respectively, and so we were able to test the hypothesis that a  $4^{\circ}\text{C}$  increase in SST would induce an acclimation response in  $T_{crit}$ .

*Statistical analyses.*  $T_{crit}$  of PSII values were extracted using breakpoint analysis of the  $T-F_0$  curves to determine the temperature at the inflection point between the slow and fast rise phases of the curve. These were assessed by fitting lines to each phase of the curve. For land plants we have R scripts to assist with this but because the kelps were relatively more variable, they were extracted manually. We assessed the repeatability of the breakpoint extraction method using three naive assessors with a subset of 30 curves from the present data and compared these to the lead authors assessment.  $R^2 = 0.92$  and on average, assessors differed by less than  $0.5^{\circ}\text{C} \pm 0.15$  to the lead authors assessment (Table S1 in the Supporting Information). See Fig. S2 in the Supporting Information for  $T_{crit}$  extraction criteria, examples, and curve variation. A small proportion of curves fail due to poor contact on the Peltier plate, fouling – which caused a relatively high proportion of failure in *Sargassum* – or low initial  $F_V/F_M$  (i.e., already stressed tissue). The supplement provides advice on how to identify these failed curves as well (Fig. S3 in the Supporting Information). We recommend practice runs to assess the best arrangement and way to get contact with the thermocouple as the proportion of failed curves decreases with time.

Linear mixed-effect models were used to investigate the decay of  $F_V/F_M$  of stored samples, with  $F_V/F_M$  as the response variable, storage time as a fixed effect and replicate as a random effect; each species was analyzed separately. Similarly, to determine the optimal saturating pulse for obtaining  $F_M$  used to calculate  $F_V/F_M$  we used linear mixed-effect models with  $F_V/F_M$  as the response variable, saturating pulse as the fixed effect and replicate as a random effect, with each species analyzed separately. To assess the effect of heating and cooling rates on the critical temperature ( $T_{crit}$ ) of PSII, linear models were used, with  $T_{crit-hot}$  or  $T_{crit-cold}$  as the response variable, heating/cooling rate treated as continuous variables and species as fixed effects. For the final experiment to determine the effect of heating/cooling with thermocouples placed above and below the sample, linear models were used similar to above but with thermocouple position as an additional fixed effect. To demonstrate the utility of  $T_{crit}$  as a comparative metric, we used a linear model with  $T_{crit}$  as the response variable and interactions between season and species as fixed effects. All analyses were performed in the stats package in R version 4.0.2 (R Core Team 2018).

## RESULTS

*Decay of  $F_V/F_M$  of stored samples from time of collection.* To determine photosynthetic physiological effects of samples removed from the water and stored, we compared the physiological response of samples to different storage methods (in wetted cotton bags vs. in seawater) over time. There was a significant interaction between storage method and time since collection for all species ( $t_{126} = 12.230$ ,  $P < 0.001$ ; Table S2 in the Supporting Information). There was no change in  $F_V/F_M$  for samples kept in wet cotton bags throughout the entire 100 h of measurements (Fig. 2). By contrast, for the samples kept in seawater,  $F_V/F_M$  began to decline substantially for *Ecklonia* and *Phyllospora* after 24 h and even earlier for *Sargassum* (10 h). There may be an effect from the initial wound during collection; however, this effect was consistent across all samples and is minimized by transporting samples in a dark cooler and measuring  $F_V/F_M$  in the center of tissue, away from the wounded edge. Therefore, because of the consistently high  $F_V/F_M$  values (the proxy for photosystem health) from the samples kept in wet cotton bags, all subsequent collections were thus made using the wet cotton bag method.

*Saturating pulse optimization using the Maxi PAM.* There was no difference in  $F_V/F_M$  as a function of saturating pulse intensity for values between PAM settings 4, 6, and 8 for both *Phyllospora* and *Sargassum*, but  $F_V/F_M$  was more variable, and generally depressed at the lowest (2) and highest (10) pulse intensities (Fig. 3a, Table S3 in the Supporting Information). *Ecklonia* showed no difference across any intensity settings. Collectively,  $F_V/F_M$  values were highest at 4 and 6. In the case of these three species, setting 4 or 6 would have been equally appropriate; we chose 6, which is approx.  $2000 \mu\text{mol quanta} \cdot \text{m}^{-2} \cdot \text{s}^{-1}$  and all following data presented are based on that setting.

*Comparison of diving PAM to Maxi PAM for measuring  $F_V/F_M$  of kelp.*  $F_V/F_M$  measurements from the Maxi PAM and Diving PAM were tightly correlated but the Maxi PAM values were on average 0.09 units lower than the Diving PAM across the range of measurements ( $\text{SE} = 0.025$ ,  $n = 85$ ; Fig. 3b). Therefore, when assessing  $F_V/F_M$  values for measurements on the Maxi PAM, adding  $\sim 0.1$  units to that output is necessary to obtain directly comparable values for those familiar with Diving PAM outputs.

*Effect of heating and cooling rates on  $T_{crit}$  of PSII of kelp species.* The heating and cooling rates affected  $T_{crit}$  when thermocouples were placed under the samples. For  $T_{crit-hot}$  we found that the critical values generally increased as heating rate increased (Fig. 4a, Table 1a). This increase with heating rate was similar between *Ecklonia* and *Phyllospora*, whereas  $T_{crit}$  of *Sargassum* was affected significantly more so, with a steeper increase with heating rate (Fig. 4a). These results suggest that ramp rates of

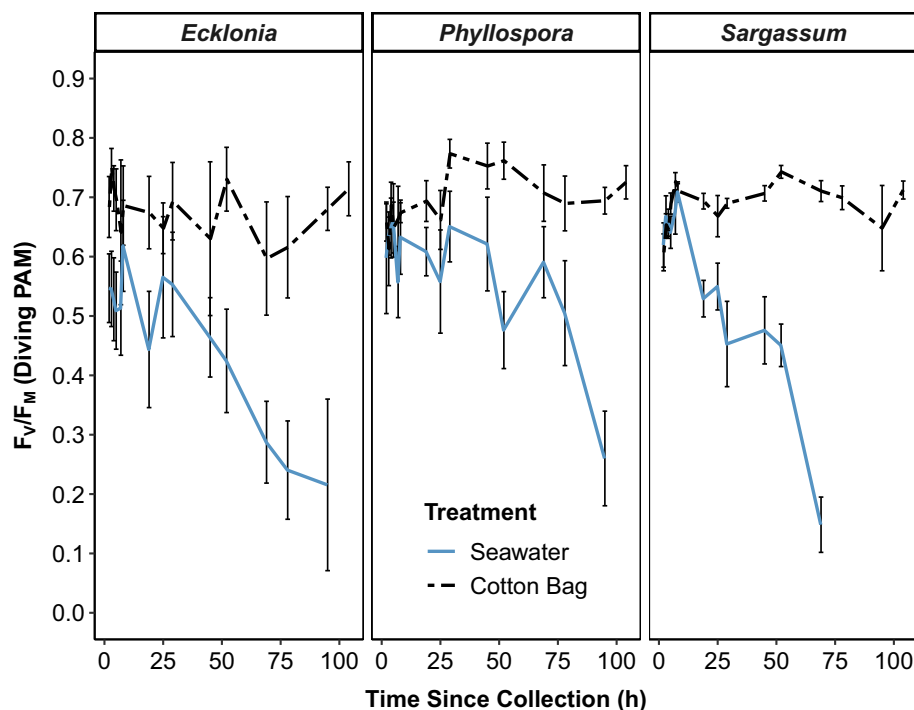


FIG. 2. Decay of maximum quantum yield ( $F_v/F_M$ ) with time since collection between two different treatments of storage: seawater (blue solid line) and in damp cotton bags (black dotted line) for three different seaweed species (*Ecklonia*, *Phyllospora* and *Sargassum*). Across all species, there was no change in  $F_v/F_M$  for samples stored in cotton bags across time, while for samples stored in seawater,  $F_v/F_M$  decline started at 25 h since collection. Points are means  $\pm$  SE,  $n = 5$  per time point per species.

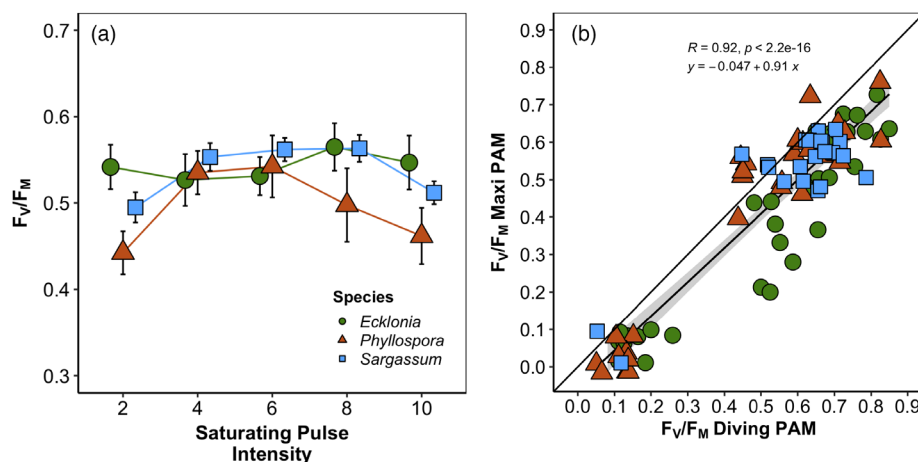


FIG. 3. Determining appropriate light levels and equipment offsets for using fluorometry on seaweeds, comparing responses of three species. (a) Optimization of saturating pulse light intensity using a Maxi PAM for each species using  $F_v/F_M$ . Pulse intensity settings 4 and 6 both showed the highest  $F_v/F_M$  with the least variation. Points are means  $\pm$  SE,  $n = 10$  per species per intensity. (b)  $F_v/F_M$  differences in output from Diving PAM versus Maxi PAM plotted with a 1:1 to show offset. Points are raw data from paired tissue across a range of samples varying in time out of water to capture entire  $F_v/F_M$  range.

15, 30, or  $45^\circ\text{C} \cdot \text{h}^{-1}$  are appropriate options for these species when measuring  $T_{\text{crit-hot}}$ . For  $T_{\text{crit-cold}}$ , overall, values became increasingly more negative at faster cooling rates, although again, there was variation among species (Fig. 4b, Table 1b). *Phyllospora* appeared virtually unaffected by changes in cooling rate, whereas  $T_{\text{crit-cold}}$  values in *Ecklonia* and

*Sargassum* were significantly affected by cooling rate as the rate increased,  $T_{\text{crit-cold}}$  became more negative (Fig. 4b).

*Heating rate artifact and modification of thermocouple placement for kelp species.* To further explain the effect of heating rate on  $T_{\text{crit-hot}}$ , we explored whether the placement of the thermocouple

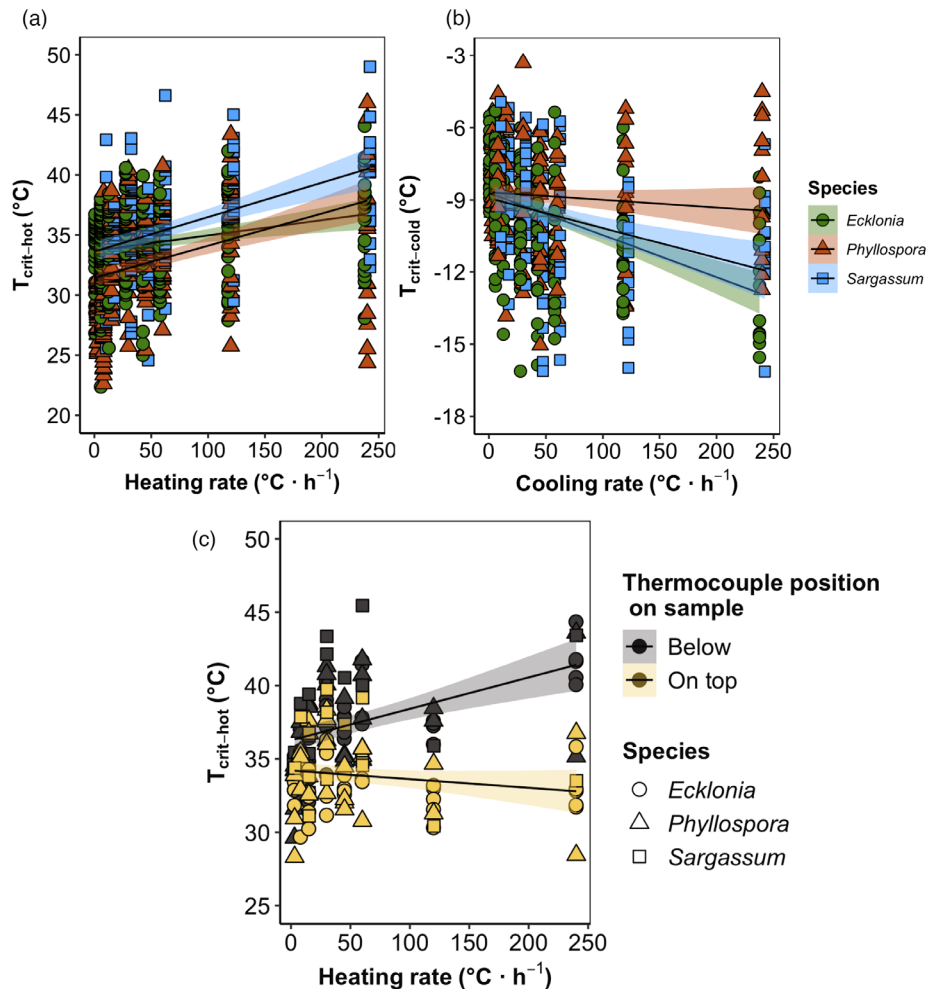


FIG. 4. Initial experiment to test heating/cooling rate on variation of  $T_{crit}$  with thermocouples on the bottom of the sample as per previous work protocols, for (a)  $T_{crit-hot}$  and (b)  $T_{crit-cold}$ . Points are means  $\pm$  SE,  $n = 30$  per species per heating/cooling rate. (c) Repeated experiment from initial heating/cooling rate variation as per (a) and (b), but with thermocouples on both top and bottom of sample for  $T_{crit-hot}$  only. The same pattern is seen with an increase in heating rate and  $T_{crit}$  when thermocouple is placed on the bottom as per previous protocols; however, with thermocouples on the top of samples,  $T_{crit-hot}$  was unaffected by heating rate.

affected the  $T_{crit-hot}$  value. When  $T_{crit-hot}$  was calculated based on a thermocouple mounted on top of the sample, there was no difference in  $T_{crit-hot}$  across any heating rate. However, the slope of  $T_{crit-hot}$  with heating rate depended on the placement of the thermocouple ( $t_{168} = -4.837$ ,  $P < 0.001$ ; Fig. 4c, Table 2). These results suggest that the high water content of large brown kelps likely serves as a thermal buffer and that thermocouples should be mounted on top of the thallus for improved measurement accuracy.

*Testing the utility of  $T_{crit}$  as a comparative metric.* Overall, the 4°C difference in SST was associated with interactions between season and species, with increases of ~3°C in  $T_{crit}$  for *Ecklonia* and *Sargassum* ( $t_{113} = 2.380$ ,  $P = 0.019$  and  $t_{113} = 2.518$ ,  $P = 0.013$ , respectively, Fig. 5) whereas *Phyllospora* showed no significant difference between the time points.

## DISCUSSION

Prior studies on seaweed thermal tolerance have applied a vast range of different methods and response variables, hindering broadscale assessments of relative vulnerability to climate change. This is in contrast to terrestrial settings where meta-analyses of consolidated datasets using comparable metrics have begun to shed light on global drivers of organismal responses to thermal stress (Bennett et al. 2018, Pinsky et al. 2019, Sunday et al. 2019, Lancaster and Humphreys 2020). To facilitate comparative thermal ecology for kelps, we modified a method from the terrestrial plant literature, temperature-dependent fluorescence curves ( $T-F_0$  curves), which we optimized using three large brown kelp species with differing morphologies. We revealed that critical temperature values can be successfully extracted from  $T-F_0$  curves for kelps and up to 48 samples



TABLE 1. Results from linear model to test for the effect of heating and cooling rates on  $T_{crit-hot}$  (a) and  $T_{crit-cold}$  (b) on each of the three species.

Predictors	$T_{crit-hot}$ estimates	CI	$P$
(a) $T_{crit-hot}$			
(Intercept)	33.42	32.63 to 34.22	<0.001***
Heating rate	0.01	0.01 to 0.02	<0.001***
Species: <i>Phyllospora</i>	-0.38	-1.52 to 0.77	0.518
Species: <i>Sargassum</i>	0.15	-1.05 to 1.35	0.807
Heating rate *	0.00	-0.01 to 0.01	0.838
Species: <i>Phyllospora</i>			
Heating rate *	0.02	0.00 to 0.03	<b>0.015*</b>
Species: <i>Sargassum</i>			
Observations	489		
$R^2/R^2$ adjusted	0.137/0.128		
Predictors	$T_{crit-cold}$ estimates	CI	$P$
(b) $T_{crit-cold}$			
(Intercept)	-9.13	-9.59 to -8.66	<0.001***
Cooling rate	-0.01	-0.02 to -0.01	<0.001***
Species: <i>Phyllospora</i>	0.24	-0.46 to 0.95	0.494
Species: <i>Sargassum</i>	-0.13	-0.88 - 0.62	0.734
Cooling rate *	0.01	0.01 to 0.02	<b>0.001***</b>
Species: <i>Phyllospora</i>			
Cooling rate *	0.00	-0.00 - 0.01	0.308
Species: <i>Sargassum</i>			
Observations	442		
$R^2/R^2$ adjusted	0.123/0.113		

Bold indicates significance at  $P < 0.05$ ; \*,  $P < 0.05$ ; \*\*,  $P < 0.01$ ; \*\*\*,  $P < 0.001$ .

TABLE 2. Results from linear model of repeated experiment to test the effect of heating rate with thermocouples on both the top and bottom of sample for each of the three species.

Predictors	$T_{crit-hot}$ estimates	CI	$P$
$T_{crit-hot}$			
(Intercept)	35.61	34.79 to 36.43	<0.001***
Thermocouple position: On top	-2.06	-3.05 to -1.08	<0.001***
Heating rate	0.02	0.01 to 0.03	<0.001***
Species: <i>Phyllospora</i>	0.62	-0.23 to 1.47	0.154
Species: <i>Sargassum</i>	2.20	1.14 to 3.25	<0.001***
Thermocouple position: On top × heating rate	-0.03	-0.04 to -0.02	<0.001***
Observations	168		
$R^2/R^2$ adjusted	0.457/0.440		

Bold indicates significance at  $P < 0.05$ ; \*,  $P < 0.05$ ; \*\*,  $P < 0.01$ ; \*\*\*,  $P < 0.001$ .

can be done in about 2 h by incorporating some important technical considerations. We observed that thermocouples positioned on top of the sample provided more accurate critical temperatures due to a reduction in thermal lag from Peltier plate to the sample. In addition, we showed that, using an appropriate storage method from time out of the water, these samples could be stored for around up to 100 h with no reduction in  $F_V/F_M$ .

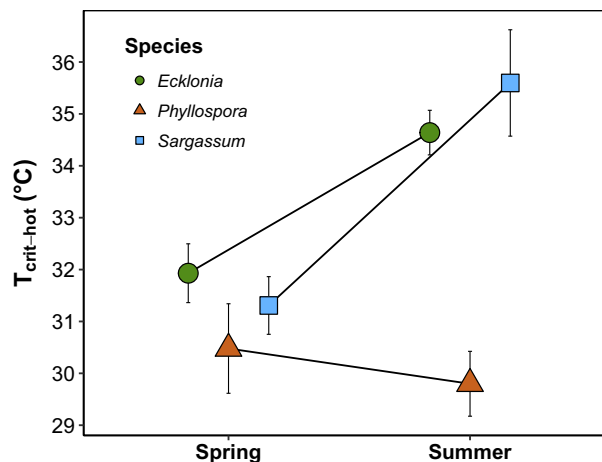


FIG. 5. Changes in  $T_{crit}$  across two seasons: Spring (October) and Summer (January) with sea surface temperature 16°C and 20°C, respectively. There was an interaction between season and species ( $P = 0.015$ ) along with a species effect ( $P < 0.001$ ) with  $T_{crit}$  increasing ~3°C in *Ecklonia* and *Sargassum*, with no change in *Phyllospora*. Points are means ± SE,  $n = 30$  per species per season.

Photosystem II and its relationship with temperature is a highly sensitive component within the photosynthetic apparatus and makes for an excellent indicator of thermal stress. Extreme temperatures can alter electron transport within PSII by increasing thylakoid membrane fluidity where the light-harvesting complex is dislodged from the thylakoid membrane (Berry and Bjorkman 1980, Srivastava et al. 1997). Because photosynthetic tissue is sensitive to temperature stress, measures of the status of photosynthetic tissue via  $F_V/F_M$  is an increasing focus of seaweed research (Pereira et al. 2015, Tan et al. 2019, Nauer et al. 2022).  $F_V/F_M$ , however, is generally only measured posttreatment, and usually in response to a range of pre-determined temperatures. These experiments tend to have a degree of subjectivity with the use of a wide range of exposure times to various temperatures, and discrepancies in both duration and intensity of the treatment, making comparisons across experiments difficult. Often these experiments are very time-consuming with long acclamatory periods, especially when using water baths, and are limited to the pre-determined temperature ranges of the experimenter and so may not capture the point of thermal stress accurately. An approach for determining critical temperatures for comparison across a range of species and environmental drivers has yet to be realized, likely because of the many logistical challenges posed by sampling marine species such as seaweeds, relative to terrestrial plants. Our approach of using temperature-dependent fluorescence ( $T-F_0$ ) curves proved to be a robust and high-throughput method that can provide a unifying metric of the photosynthetic thermal tolerance of kelp species, with potential for wide-scale ecological screening of thermal

tolerance.  $T-F_0$  curves provide an easily applied method to extract critical temperatures ( $T_{\text{crit}}$ ) of PSII (i.e., changes in energy conversion and excitation within PSII from chlorophyll *a* fluorescence), which we found to be successful across all kelp species we measured. We were able to quantify  $T_{\text{crit}}$  from 30 individuals in a single assay (with maximum of up to 48, depending on datalogger capacity) at a rate of  $15^{\circ}\text{C} \cdot \text{h}^{-1}$  in just over 2.5 h, or  $1.5^{\circ}\text{C} \cdot \text{h}^{-1}$  from the time samples were dark-adapted to the end of the assay. We found no dependence on heating/cooling rate as opposed to previous methods, particularly  $F_V/F_M$  whose results vary widely depending on the temperature, exposure time, duration, and intensity of the imposed treatment within the experiment.  $T-F_0$  curves provide a robust comparative metric, offering very high throughput and the applications of this technique for future experimental and ecological surveys will allow physiological thresholds to be compared species, space, time, and varying experimental conditions. We note that this method is yet to be tested on Rhodophyta and Chlorophyta species. However, with careful consideration of species pigment composition – these classes also have chlorophyll *a* that dominates fluorescence, particularly at 450 nm, which is also the wavelength that the PAM uses (Schreiber et al. 2012, Preuss and Zuccarello 2019) – and the calibration of the PAM light source used,  $T-F_0$  curves are likely to also prove useful to these classes and broaden the applications of the technique and progress the field of algal research.

As is the case for terrestrial plants (Zhu et al. 2018, Arnold et al. 2021), values of thermal tolerance from our study suggest the photosystems of seaweeds can function at higher temperatures than their ambient environment (e.g.,  $T_{\text{crit}}$  of  $33^{\circ}\text{C}$  in summer for *Ecklonia* and *Phyllospora*, and  $35^{\circ}\text{C}$  for *Sargassum* with ambient sea surface temperatures only being  $\sim 20^{\circ}\text{C}$ ). For example, *Ecklonia* thermal thresholds in the field occur at temperatures much lower than  $33^{\circ}\text{C}$  (plants generally die at  $\sim 27^{\circ}\text{C}$ ; Wernberg et al. 2019). We note that the relative  $T_{\text{crit}}$  of PSII values for the three species we tested here generally followed expectations of thermal tolerance and persistence from the field, with the widely distributed *Sargassum* having higher  $T_{\text{crit-hot}}$  and the cooler-water *Phyllospora* having a more negative  $T_{\text{crit-cold}}$ . PSII thermostability is occurring within the thylakoid membrane from excised tissue, and the values derived from  $T_{\text{crit}}$  cannot be scaled to the whole plant level. In the natural environment, such thermal stress occurs in conjunction with light and other stressors that culminate to lower the realized thermal thresholds for species survival (Lobban and Harrison 1994, Altamirano et al. 2004). Such a complexity of stressors that can be unique to species and places are impossible to emulate in experimental settings making direct comparisons of thermal thresholds difficult. The methods presented here

negate this issue by presenting a standard method that can be applied across photosynthetic organisms. Here, we were not aiming to emulate the natural environment but to propose a standardized method that enables a metric for researchers to compare instantaneous  $T_{\text{crit}}$  across species and spatial scales. It is likely that with light stress combined with thermal stress, these critical values may occur at lower temperatures, but this is not logistically feasible to measure  $T_{\text{crit}}$  during illumination; however, these protocols allow for the metric to be comparative. Thus, rather than using the absolute value of  $T_{\text{crit}}$  of PSII to signify when species will cease to persist in natural environments, the critical threshold has greatest utility as a relative value. When comparing among species, populations, and seasons for example, these thresholds become useful indicators of thermal tolerance where patterns match or deviate from one another. An excellent example of the ecological relevance and application of  $T_{\text{crit}}$  of PSII is in O'Sullivan et al. (2017). The absolute latitude and the mean maximum temperature of the warmest month were both significantly correlated with  $T_{\text{crit-hot}}$  for 218 terrestrial plant species across seven different biomes. The authors found a  $10^{\circ}\text{C}$  increase in  $T_{\text{crit-hot}}$  from the Arctic to the Amazon rainforest, with mid-latitude regions having the narrowest thermal safety margins (defined as the difference between  $T_{\text{crit-hot}}$  and experienced leaf temperature during extreme weather events). They were able to use their dataset in a 2050 climate scenario and found these thermal safety margins would likely shrink as temperatures begin to exceed thermal tolerance limits, identifying specific biomes more at risk to severe weather events than others.

*Optimizing T-F<sub>0</sub> method for seaweeds.* Various parameters needed to be optimized for use with seaweeds, including maintaining sample tissue integrity through optimal storage following removal of samples from the ocean and thermocouple placement during measurements. First, our results indicate that when stored appropriately post-collection, samples are robust for this method. Samples kept in damp cotton bags, rather than submerged in seawater, maintained optimal photosynthetic function for several days. We do not advocate storing samples for longer than 100 h, but one can certainly collect samples in the field and return samples to the laboratory for assays within a day or two if in a remote area.

We also identified that several modifications must be made to transition the  $T-F_0$  method from terrestrial plants to seaweeds. While we initially placed thermocouples below the samples as per protocols used for terrestrial leaves (Bilger et al. 1984, Frolec et al. 2008, Arnold et al. 2021), our results demonstrate how heating and cooling rates can significantly affect  $T_{\text{crit}}$  estimates in our chosen species. This could be an artifact of delayed heating of the sample from the heating element to the top of the

sample due to morphology, or an actual physiological response to a faster rate. We sought to tease this apart by measuring the critical temperature ( $T_{\text{crit-hot}}$ ) both above and below the sample on the heating element, finding a large difference between the two surfaces. Part of our methods optimization was to test this on species with variation in thallus morphology, and we found the large differences in  $T_{\text{crit}}$  were exacerbated by increased thickness of the sample (i.e., the higher water content and thicker medullary cell layers of *Phyllospora* and *Ecklonia* compared to *Sargassum*; Bell 1993, Lobban and Harrison 1994) led to a greater difference in temperature between surfaces in these species, which was enhanced by an increase in heating/cooling rate (Fig. 4c). When thermocouples were placed on the top of the sample, there was no evidence of a thermal lag artifact whatsoever, regardless of temperature ramp rate. Though water in plant tissue heats uniformly, it heats slowly (Leigh et al. 2012), so we highly recommend placing thermocouples on top of seaweed samples as standard practice, rather than underneath. Only at very slow heating/cooling rates ( $3\text{--}8^{\circ}\text{C} \cdot \text{h}^{-1}$ ) was the temperature difference between top and bottom thermocouples minimal (only about  $1\text{--}2^{\circ}\text{C}$ ) and, therefore, could be ignored. But we caution that such slow rates may invoke other artifacts; for example, samples exposed to high temperatures for a much longer period of time may induce acclamatory or stress responses.

It is essential that heating and cooling rates are selected appropriately based on a trade-off between high sample throughput and accuracy. We measured heating and cooling rates up to  $240^{\circ}\text{C} \cdot \text{h}^{-1}$ , but do not generally recommend using such rates, given that the sample will have a temperature gradient and will lead to less reliable  $T_{\text{crit}}$  values. We recommend a relatively slow, yet convenient rate of  $15^{\circ}\text{C} \cdot \text{h}^{-1}$  or  $30^{\circ}\text{C} \cdot \text{h}^{-1}$ , which takes about 1–2 h to complete for 30–48 samples. Including time for sample preparation, placement and dark adaptation, the full assay would take just 3 and 2 h for 15 and  $30^{\circ}\text{C} \cdot \text{h}^{-1}$ , respectively. A slower heating/cooling rate also allows for increased accuracy in the breakpoint analysis for the experimenter. At  $15^{\circ}\text{C} \cdot \text{h}^{-1}$  the temperature change at the point of fast rise of  $F_0$  remains within a difference of less than  $1^{\circ}\text{C}$ , with minimal temperature change during breakpoint selection.

Various settings on the Peltier controller software can be adjusted, such as application of temperature treatments as a specific temperature shock, different heating or cooling rates, or in specific stepwise increments. In addition to  $T_{\text{crit}}$ ,  $T_{50}$  (temperature at 50% fluorescence peak  $F_0$  fluorescence), and  $T_{\text{max}}$  (temperature at maximum  $F_0$ ) are also outputs available from the  $T\text{--}F_0$  curve, broadening the metrics and their uses. For example, terrestrial plant physiologists have used  $T_{\text{crit}}$ ,  $T_{\text{max}}$ ,  $T_{20}$ , and  $T_{50}$  to predict photosynthetic thermal tolerance decline across a

huge range of species, biomes, and treatments with some parameters better predicting decline than others (Knight and Ackerly 2002, Tarvainen et al. 2021).

Researchers will need to optimize the arrangement of samples to account for variation in seaweed morphologies and variation among individuals. The  $T\text{--}F_0$  method was robust to measuring these three species with different thicknesses in the same assay, but thickness varies greatly in other species and needs to be considered. For example, a genus with a thick thallus such as *Durvillaea* should not be assayed alongside a thin *Sargassum*. Moreover, individuals of the same species with vastly different thallus thicknesses should be tested separately. The  $T\text{--}F_0$  method relies on good contact and minimal air gaps between the glass, plastic-wrap, thermocouples, and samples. If contact between the samples and the glass is poor, then the insulative properties of the glass will be diminished and the sample will not maintain a uniform temperature, which would overestimate  $T_{\text{crit}}$  of PSII. Therefore, we recommend that a single assay of up to 48 samples of similar thickness be done per plate. For experimenters wishing to employ this method on other species, we recommend they screen a subset of individuals beforehand. Being aware of the growth cycles, wounding responses, morphologies, pigment composition, and to optimize use of the PAM for the target species will reduce the likelihood of failed  $T\text{--}F_0$  curves and increase the reliability and repeatability of the data.

*Future directions.* As we have demonstrated here,  $T\text{--}F_0$  curves can detect seasonal changes and species level differences in thermal tolerance and acclimation thereof. Given this, we advocate using these as a standardized unifying metric to advance thermal physiology. We advocate temperature-dependent fluorescence curves to derive  $T_{\text{crit}}$  of PSII as an exciting tool to assess and compare photosynthetic thermal tolerance of seaweeds. Its standardized output and high-throughput ability make it possible to rapidly assay thermal tolerance across many populations and species across the globe. Cross-species comparisons of critical temperatures would enable better predictions of how community composition could change as a function of changing sea surface temperature. This method also allows for the calculation and comparison of thermal safety margins, a measure of how close thermal tolerance is to the actual maximum sea temperature, which is a common metric used to delineate plant species at risk under climate change (O'Sullivan et al. 2017). In addition, within-species assessment of variation in critical temperatures along latitudinal gradients would provide insight about the extent of local adaptation in thermal physiology. Assays of temporal (e.g., among seasons) and spatial (e.g., thermal depth gradients) differences in  $T_{\text{crit}}$  on a population would aid predictions of relative acclimation

potential or range shifts under climate change. Finally, pairing these phenotypic assays with measures of genetic differentiation or patterns of gene expression would provide powerful potential for mechanistic insight into what confers thermal tolerance in seaweeds. Such studies have implications for conservation and restoration work as well as for our fundamental understanding of the evolution of thermal physiology in photosynthetic organisms.

We respectfully acknowledge the Yuin and Ngunnawal First Nations peoples as the Traditional Custodians of the lands where this research took place. This research was supported by the Ecological Society of Australia through The Holsworth Wildlife Research Endowment, The Linnean Society of NSW through the Joyce W Vickery Scientific Research Fund and by the Australian Government Research Training Program, each awarded to R Harris. We thank Peter Ralph, Executive Director of the C3 Research Institute, UTS, for invaluable early discussions on logistical considerations and the UTS Faculty of Science for technical support with the Diving PAM. Seaweed samples were collected under NSW Department of Primary Industries Scientific Collection Permit number: P01/0059(A)-3.0. The authors declare no conflict of interest. Open access publishing facilitated by Australian National University, as part of the Wiley - Australian National University agreement via the Council of Australian University Librarians.

- Alam, T. 2019. Extraction of natural colors from marine algae. *J. Agric. Mar. Sci. JAMS* 23:81.
- Allakhverdiev, S. I., Kreslavski, V. D., Klimov, V. V., Los, D. A., Carpentier, R. & Mohanty, P. 2008. Heat stress: an overview of molecular responses in photosynthesis. *Photosynth. Res.* 98:541–50.
- Altamirano, M., Murakami, A. & Kawai, H. 2004. High light stress in the kelp *Ecklonia cava*. *Aquat. Bot.* 79:125–35.
- Arnold, P. A., Briceño, V. F., Gowland, K. M., Catling, A. A., Bravo, L. A. & Nicotra, A. B. 2021. A high-throughput method for measuring critical thermal limits of leaves by chlorophyll imaging fluorescence. *Funct. Plant Biol.* 48:634–46.
- Becker, S., Walter, B. & Bischof, K. 2009. Freezing tolerance and photosynthetic performance of polar seaweeds at low temperatures. *Bot. Mar.* 52:609–16.
- Bell, E. C. 1993. Photosynthetic response to temperature and desiccation of the intertidal alga *Mastocarpus papillatus*. *Mar. Biol.* 117:337–46.
- Bennett, J. M., Calosi, P., Clusella-Trullas, S., Martínez, B., Sunday, J., Algar, A. C., Araújo, M. B. et al. 2018. GlobTherm, a global database on thermal tolerances for aquatic and terrestrial organisms. *Sci. Data* 5:1–7.
- Berry, J. & Bjorkman, O. 1980. Photosynthetic response and adaptation to temperature in higher plants. *Annu. Rev. Plant Physiol.* 31:491–543.
- Bilger, H. W., Schreiber, U. & Lange, O. L. 1984. Determination of leaf heat resistance: comparative investigation of chlorophyll fluorescence changes and tissue necrosis methods. *Oecologia* 63:256–62.
- Cabello-Pasini, A., Aguirre-von-Wobeser, E. & Figueroa, F. L. 2000. Photoinhibition of photosynthesis in *Macrocystis pyrifera* (Phaeophyceae), *Chondrus crispus* (Rhodophyceae) and *Ulva lactuca* (Chlorophyceae) in outdoor culture systems. *J. Photochem. Photobiol. B* 57:169–78.
- Caetano, G. H. O., Santos, J. C., Godinho, L. B., Cavalcante, V. H. G. L., Diele-Viegas, L. M., Campelo, P. H., Martins, L. F. et al. 2020. Time of activity is a better predictor of the distribution of a tropical lizard than pure environmental temperatures. *Oikos* 129:953–63.
- Caron, L., Douady, D., Martino, A. D. & Quinet, M. 2001. Light harvesting in brown algae. *Cah. Biol. Mar.* 42:109–24.
- Cavanaugh, K. C., Reed, D. C., Bell, T. W., Castorani, M. C. N. & Beas-Luna, R. 2019. Spatial variability in the resistance and resilience of giant kelp in Southern and Baja California to a multiyear heatwave. *Front. Mar. Sci.* 6:413.
- Coleman, M. A. & Wernberg, T. 2017. Forgotten underwater forests: the key role of fucoids on Australian temperate reefs. *Ecol. Evol.* 7:8406–18.
- Coleman, M. A. & Wernberg, T. 2020. The silver lining of extreme events. *Trends Ecol. Evol.* 35:1065–7.
- Curtis, E. M., Gollan, J., Murray, B. R. & Leigh, A. 2016. Native microhabitats better predict tolerance to warming than latitudinal macro-climatic variables in arid-zone plants. *J. Biogeogr.* 43:1156–65.
- Davis, T. R., Champion, C. & Coleman, M. A. 2022. Ecological interactions mediate projected loss of kelp biomass under climate change. *Divers. Distrib.* 28:306–17.
- Davison, I., Dudgeon, S. & Ruan, H.-M. 1989. Effect of freezing on seaweed photosynthesis. *Mar. Ecol. Prog. Ser.* 58:123–31.
- Djaeni, M. & Sari, D. A. 2015. Low temperature seaweed drying using dehumidified air. *Proc. Environ. Sci.* 23:2–10.
- Eger, A. M., Marzini, E. M., Christie, H., Fagerli, C. W., Fujita, D., Gonzalez, A. P., Hong, S. W. et al. 2022. Global kelp forest restoration: past lessons, present status, and future directions. *Biol. Rev.* 97:1449–75.
- Enami, I., Kitamura, M., Tomo, T., Isokawa, Y., Ohta, H. & Katoh, S. 1994. Is the primary cause of thermal inactivation of oxygen evolution in spinach PS II membranes release of the extrinsic 33 kDa protein or of Mn? *Biochim. Biophys. Acta BBA - Bioenerg.* 1186:52–8.
- Enríquez, S. & Borowitzka, M. A. 2010. The use of the fluorescence signal in studies of seagrasses and macroalgae. *Chlorophyll Fluoresc. Aquat. Sci. Methods Appl.* 4:187–208.
- Etemadian, Y. 2017. Compare the chlorophyll amount in three brown algae species of the Persian Gulf by using three solvents and applying two formulas. *Int. J. Biochem. Biophys. Mol. Biol.* 2:77.
- Fernández, P. A., Gaitán-Espitia, J. D., Leal, P. P., Schmid, M., Revill, A. T. & Hurd, C. L. 2020. Nitrogen sufficiency enhances thermal tolerance in habitat-forming kelp: implications for acclimation under thermal stress. *Sci. Rep.* 10:3186.
- Frolec, J., Ilík, P., Krchňák, P., Sušila, P. & Naus, J. 2008. Irreversible changes in barley leaf chlorophyll fluorescence detected by the fluorescence temperature curve in a linear heating/cooling regime. *Photosynthetica* 46:537–46.
- Geange, S. R., Arnold, P. A., Catling, A. A., Coast, O., Cook, A. M., Gowland, K. M., Leigh, A. et al. 2021. The thermal tolerance of photosynthetic tissues: a global systematic review and agenda for future research. *New Phytol.* 229:2497–513.
- Hall, J. M. & Sun, B. 2021. Heat tolerance of reptile embryos: current knowledge, methodological considerations, and future directions. *J. Exp. Zool. Part Ecol. Integr. Physiol.* 335:45–58.
- Harley, C. D. G., Anderson, K. M., Demes, K. W., Jorve, J. P., Kordas, R. L., Coyle, T. A. & Graham, M. H. 2012. Effects of climate change on global seaweed communities. *J. Phycol.* 48:1064–78.
- Holbrook, N. J., Sen Gupta, A., Oliver, E. C. J., Hobday, A. J., Benthuisen, J. A., Scannell, H. A., Smale, D. A. & Wernberg, T. 2020. Keeping pace with marine heatwaves. *Nat. Rev. Earth Environ.* 1:482–93.
- Hüve, K., Bichele, I., Tobias, M. & Niinemets, Ü. 2006. Heat sensitivity of photosynthetic electron transport varies during the day due to changes in sugars and osmotic potential. *Plant Cell Environ.* 29:212–28.
- Ilík, P., Kouřil, R., Kruk, J., Strza, K., Myśliwa-Kurczel, B., Popelková, H., Strzałka, K. & Naus, J. 2003. Origin of chlorophyll fluorescence in plants at 55–75°C. *Photochem. Photobiol.* 77:68–76.
- IPCC 2021. *Working Group I Contribution to the Sixth Assessment Report of the Intergovernmental Panel on Climate Change*. Cambridge University Press, Cambridge, UK, 13 pp.

- Johnson, C. R., Banks, S. C., Barrett, N. S., Cazassus, F., Dunstan, P. K., Edgar, G. J., Frusher, S. D. et al. 2011. Climate change cascades: Shifts in oceanography, species' ranges and subtidal marine community dynamics in eastern Tasmania. *J. Exp. Mar. Biol. Ecol.* 400:17–32.
- Knight, C. A. & Ackerly, D. D. 2002. An ecological and evolutionary analysis of photosynthetic thermotolerance using the temperature-dependent increase in fluorescence. *Oecologia* 130:505–14.
- Krause, G. H., Winter, K., Krause, B., Jahns, P., García, M., Aranda, J. & Virgo, A. 2010. High-temperature tolerance of a tropical tree, *Ficus insipida*: methodological reassessment and climate change considerations. *Funct. Plant Biol.* 37:890–900.
- Lancaster, L. T. & Humphreys, A. M. 2020. Global variation in the thermal tolerances of plants. *Proc. Natl. Acad. Sci. USA* 117:13580–7.
- Leigh, A., Sevanto, S., Ball, M. C., Close, J. D., Ellsworth, D. S., Knight, C. A., Nicotra, A. B. & Vogel, S. 2012. Do thick leaves avoid thermal damage in critically low wind speeds? *New Phytol.* 194:477–87.
- Lobban, C. S. & Harrison, P. J. 1994. *Seaweed ecology and physiology*. Cambridge University Press, Cambridge, UK, 388 pp.
- López-Cristoffanini, C., Zapata, J., Gaillard, F., Potin, P., Correa, J. A. & Contreras-Porcía, L. 2015. Identification of proteins involved in desiccation tolerance in the red seaweed *Pyropia orbicularis* (Rhodophyta, Bangiales). *Proteomics* 15:3954–68.
- Maxwell, K. & Johnson, G. N. 2000. Chlorophyll fluorescence—a practical guide. *J. Exp. Bot.* 51:659–68.
- Nauer, F., Oliveira, M. C., Plastino, E. M., Yokoya, N. S. & Fujii, M. T. 2022. Coping with heatwaves: how a key species of seaweed responds to heat stress along its latitudinal gradient. *Mar. Environ. Res.* 177:105620.
- Oliver, E. C. J., Donat, M. G., Burrows, M. T., Moore, P. J., Smale, D. A., Alexander, L. V., Benthuisen, J. A. et al. 2018. Longer and more frequent marine heatwaves over the past century. *Nat. Commun.* 9:1324.
- O'Sullivan, O. S., Heskell, M. A., Reich, P. B., Tjoelker, M. G., Weerasinghe, L. K., Penillard, A., Zhu, L. et al. 2017. Thermal limits of leaf metabolism across biomes. *Glob. Change Biol.* 23:209–23.
- Papageorgiou, G. C., Tsimilli-Michael, M. & Stamatakis, K. 2007. The fast and slow kinetics of chlorophyll a fluorescence induction in plants, algae and cyanobacteria: a viewpoint. *Photosynth. Res.* 94:275–90.
- Pereira, T. R., Engelen, A. H., Pearson, G. A., Valero, M. & Serrão, E. A. 2015. Response of kelps from different latitudes to consecutive heat shock. *J. Exp. Mar. Biol. Ecol.* 463:57–62.
- Pinsky, M. L., Eikeset, A. M., McCauley, D. J., Payne, J. L. & Sunday, J. M. 2019. Greater vulnerability to warming of marine versus terrestrial ectotherms. *Nature* 569:108–11.
- Preuss, M. & Zuccarello, G. C. 2019. Comparative studies of photosynthetic capacity in three pigmented red algal parasites: Chlorophyll a concentrations and PAM fluorometry measurements. *Phycol. Res.* 67:89–93.
- R Core Team 2018. *R: A Language and Environment for Statistical Computing*. R Foundation for Statistical Computing, Vienna, 12 p.
- Roze, T., Christen, F., Amerand, A. & Claireaux, G. 2013. Trade-off between thermal sensitivity, hypoxia tolerance and growth in fish. *J. Therm. Biol.* 38:98–106.
- Sava, I., Bennett, S., Roca, G., Jordà, G. & Marbà, N. 2018. Thermal tolerance of Mediterranean marine macrophytes: vulnerability to global warming. *Ecol. Evol.* 8:12032–43.
- Schreiber, U. & Berry, J. A. 1977. Heat-induced changes of chlorophyll fluorescence in intact leaves correlated with damage of the photosynthetic apparatus. *Planta* 136:233–8.
- Schreiber, U. & Bilger, W. 1987. Rapid assessment of stress effects on plant leaves by chlorophyll fluorescence measurements. *Plant Res. Str.* 15:27–53.
- Schreiber, U., Klughammer, C. & Kolbowski, J. 2012. Assessment of wavelength-dependent parameters of photosynthetic electron transport with a new type of multi-color PAM chlorophyll fluorometer. *Photosynth. Res.* 113:127–44.
- Scrosati, R. A. & Ellich, J. A. 2018. Thermal moderation of the intertidal zone by seaweed canopies in winter. *Mar. Biol.* 165:115.
- Srivastava, A., Guissé, B., Greppin, H. & Strasser, R. J. 1997. Regulation of antenna structure and electron transport in Photosystem II of *Pisum sativum* under elevated temperature probed by the fast polyphasic chlorophyll a fluorescence transient: OKJIP. *Biochim. Biophys. Acta BBA – Bioenerg.* 1320:95–106.
- Sunday, J., Bennett, J. M., Calosi, P., Clusella-Trullas, S., Gravel, S., Hargreaves, A. L., Leiva, F. P., Verberk, W. C. E. P., Olalla-Tárraga, M. Á. & Morales-Castilla, I. 2019. Thermal tolerance patterns across latitude and elevation. *Philos. Trans. R. Soc. B Biol. Sci.* 374:20190036.
- Sunday, J. M., Bates, A. E. & Dulvy, N. K. 2011. Global analysis of thermal tolerance and latitude in ectotherms. *Proc. R. Soc. B Biol. Sci.* 278:1823–30.
- Sunny, A. R. 2017. A review on effect of global climate change on seaweed and seagrass. *Int. J. Fish. Aquat. Stud.* 5:19–22.
- Tan, L., Xu, W., He, X. & Wang, J. 2019. The feasibility of Fv/Fm on judging nutrient limitation of marine algae through indoor simulation and in situ experiment. *Estuar. Coast. Shelf Sci.* 229:106411.
- Tarvainen, L., Wittmann, M., Mujawamariya, M., Manishimwe, A., Zibera, E., Ntirugulirwa, B., Ract, C. et al. 2021. Handling the heat – photosynthetic thermal stress in tropical trees. *New Phytol.* 233:236–50.
- Thomsen, M. S., Mondardini, L., Alestra, T., Gerrity, S., Tait, L., South, P. M., Lilley, S. A. & Schiel, D. R. 2019. Local extinction of bull kelp (*Durvillaea* spp.) due to a marine heatwave. *Front. Mar. Sci.* 6:84.
- Vergés, A., Doropoulos, C., Malcolm, H. A., Skye, M., Garcia-Pizá, M., Marzinelli, E. M., Campbell, A. H. et al. 2016. Long-term empirical evidence of ocean warming leading to tropicalization of fish communities, increased herbivory, and loss of kelp. *Proc. Natl. Acad. Sci. USA* 113:13791–6.
- Vergés, A., Steinberg, P. D., Hay, M. E., Poore, A. G. B., Campbell, A. H., Ballesteros, E., Heck, K. L. et al. 2014. The tropicalization of temperate marine ecosystems: climate-mediated changes in herbivory and community phase shifts. *Proc. R. Soc. B Biol. Sci.* 281:20140846.
- Wernberg, T., Bennett, S., Babcock, R. C., de Bettignies, T., Cure, K., Depczynski, M., Dufois, F. et al. 2016. Climate-driven regime shift of a temperate marine ecosystem. *Science* 353:169–72.
- Wernberg, T., Coleman, M. A., Babcock, R. C., Bell, S. Y., Bolton, J. J., Connell, S. D., Hurd, C. L. et al. 2019. Chapter 6 Biology and ecology of the globally significant kelp *Ecklonia radiata*. In Hawkins, S. J., Allcock, A. L., Bates, A. E., Firth, L. B., Smith, I. P., Swearer, S. E. & Todd, P. A. [Eds.] *Oceanography and Marine Biology*. Taylor & Francis, Abingdon-on-Tames, UK, pp. 265–324.
- Wood, G., Marzinelli, E. M., Campbell, A. H., Steinberg, P. D., Vergés, A. & Coleman, M. A. 2021. Genomic vulnerability of a dominant seaweed points to future-proofing pathways for Australia's underwater forests. *Glob. Change Biol.* 27:2200–12.
- Xiao, X., de Bettignies, T., Olsen, Y. S., Agustí, S., Duarte, C. M. & Wernberg, T. 2015. Sensitivity and acclimation of three canopy-forming seaweeds to UVB radiation and warming. *PLoS ONE* 10:e0143031.
- Yamane, Y., Kashino, Y., Koike, H. & Satoh, K. 1997. Effects of high temperatures on the photosynthetic systems in spinach: oxygen-evolving activities, fluorescence characteristics and the denaturation process. *Photosynth. Res.* 57:51–9.
- Zhu, L., Bloomfield, K. J., Hocart, C. H., Egerton, J. J. G., O'Sullivan, O. S., Penillard, A., Weerasinghe, L. K. & Atkin, O. K. 2018. Plasticity of photosynthetic heat tolerance in plants adapted to thermally contrasting biomes. *Plant Cell Environ.* 41:1251–62.



Zhu, S., Gu, D., Lu, C., Zhang, C., Chen, J., Yang, R., Luo, Q., Wang, T., Zhang, P. & Chen, H. 2022. Cold stress tolerance of the intertidal red alga *Neoporphyra haitanensis*. *BMC Plant Biol.* 22:114.

### Supporting Information

Additional Supporting Information may be found in the online version of this article at the publisher's web site:

**Figure S1.** Decline of  $F_V/F_M$  of samples kept in pillboxes (for storage while preparing experiments) through time.

**Figure S2.** Examples of common types of  $T-F_0$  curves encountered in breakpoint analysis of temperature-dependent changes in chlorophyll fluorescence in seaweed photosynthetic tissues to obtain  $T_{crit}$ .

**Figure S3.** Examples of the shapes of fluorescence curves that experimenter should remove from further analysis.

**Table S1.** Results from a linear mixed-effects model to test the effects of three independent assessors on  $T_{crit}$  compared to lead authors extractions of  $T_{crit}$ .

**Table S2.** Results of linear mixed-effects models of the decay of  $F_V/F_M$  of stored samples from time of collection.

**Table S3.** Saturating pulse optimization experiment to determine optimum flash for the three species collectively using  $F_V/F_M$ .